The Vinculin/Sarcomeric-α-Actinin/α-Actin Nexus in Cultured Cardiac Myocytes

Mei-Hua Lu,*‡ Camille DiLullo,* Thomas Schultheiss,§ Sybil Holtzer,* John M. Murray,* John Choi,* Donald A. Fischman,‖ and Howard Holtzer*

*Department of Anatomy, University of Pennsylvania Medical School, Philadelphia, Pennsylvania 19104-6058; ‡Department of Biology and Anatomy, National Defense Medical Center, Taipei, Taiwan; §Department of Pathology, Brigham and Women's Hospital, Boston, Massachusetts 02115; and ‖Department of Cell Biology and Anatomy, Cornell University Medical College, New York 10021

Abstract. Experiments are described supporting the proposition that the assembly of stress fibers in non-muscle cells and the assembly of myofibrils in cardiac cells share conserved mechanisms. Double staining with a battery of labeled antibodies against membrane-associated proteins, myofibrillar proteins, and stress fiber proteins reveals the following: (*a*) dissociated, cultured cardiac myocytes reconstitute intercalated discs consisting of adherens junctions (AJs) and desmosomes at sites of cell–cell contact and sub-sarcolemmal adhesion plaques (SAPs) at sites of cell–substrate contact; (*b*) each AJ or SAP associates proximally with a striated myofibril, and conversely every striated myofibril is capped at either end by an AJ or a SAP; (*C*) the invariant association between a given myofibril and its SAP is especially prominent at the earliest stages of myofibrillogenesis; nascent myofibrils are capped by oppositely oriented SAPs; (*d*) the insertion of nascent myofibrils into AJs or into SAPs invariably involves vinculin, α-actin, and sarcomeric α-actinin (s–α-actinin); (*e*) AJs are positive for A-CAM but negative for talin and integrin; SAPs lack A-CAM but are positive for talin and integrin; (*f*) in cardiac cells all α-actinin–containing structures invariably are positive for the sarcomeric isoform, α-actin and related sarcomeric proteins; they lack non-s–α-actinin, γ-actin, and caldesmon; (*g*) in fibroblasts all α-actinin–containing structures are positive for the non-sarcomeric isoform, γ-actin, and related non-sarcomeric proteins, including caldesmon; and (*h*) myocytes differ from all other types of adherent cultured cells in that they do not assemble authentic stress fibers; instead they assemble stress fiber–like structures of linearly aligned I-Z-I–like complexes consisting exclusively of sarcomeric proteins.

CONSIDERABLE information has accumulated regarding the molecular composition and possible functions of the submembranous complexes into which stress fibers insert (4, 5, 11, 26, 34, 46). In cell–cell junctions of the adherens type the distal tips of the microfilament bundles insert into submembranous F-actin/α-actinin/vinculin complexes that often involve additional membrane-associated molecules such as A-CAM (31, 60), radixin (58) etc. A somewhat different class of submembranous complexes characterizes the termini of stress fibers where they insert into the cell–substrate junctions of spread, nontranslocating cultured cells. These F-actin/α-actinin/vinculin complexes, known as adhesion plaques (APs),[1] are also positive for talin (11), paxillin (59), integrin (17), and other proteins. APs are also sites for a Ca²⁺-dependent protease (5) and a

protein kinase C (35) suggesting they may be involved in transmembrane signaling. In both the adherens junction (AJs) and the APs, α-actinin appears to play a bifunctional role. Distally, facing the inner surface of the cell membrane, α-actinin forms complexes with vinculin and other membrane-associated molecules (46); proximally, facing the cytoplasm, α-actinin forms complexes with F-actin, caldesmon (9, 20), and other nonsarcomeric contractile proteins that make up stress fibers. The theme of submembranous F-actin/α-actinin/vinculin complexes is also expressed in mature heart cells. In vivo cardiac myocytes assemble numerous longitudinally oriented myofibrils which insert into AJs of intercalated discs (10, 24, 26, 28, 60). Each insertion site is characterized by a prominent F-actin/α-actinin/vinculin plaque. Still to be determined are: (*a*) whether during development there is a switch in either AJs or subsarcolemmal adhesion plaques (SAPs) from β- and γ-actin to α-actin, and from non-sarcomeric(s)–α-actinin to s–α-actinin; and (*b*) if such a switch occurs how this correlates temporally and spatially with the assembly of nascent myofibrils.

---

1. *Abbreviations used in this paper*: AJ, adherens junction; AP, adhesion plaque; MHC, myosin heavy chain; s, sarcomeric; SAP, subsarcolemmal adhesion plaque.

Recently two reports have enlarged on similarities between the behavior and spatial distribution of stress fibers and their associated APs in cultured nonmuscle cells on one hand and of myofibrils and their associated SAPs in cultured cardiac cells on the other. Lin et al. (42) and Schultheiss et al. (54) reported that dissociated embryonic chick cardiac myocytes sequentially disassemble their striated myofibrils, forming numerous transitory polygons (see also 29, 55). The cardiac polygons are analogous to the stress fiber polygons in spread nonmuscle cells (39). They differ from their counterparts in nonmuscle cells in that the muscle polygons consist of s-α-actinin vertices and s-MHC struts rather than of the corresponding nonsarcomeric isoforms as in stress-fiber polygons. Concurrent with the disassembly and elimination of the original myofibrils, a new population of myofibrils is assembled elsewhere in the same myocyte. The distal tips of these de novo–assembled myofibrils insert into SAPs that morphologically are similar to the APs capping the termini of stress fibers in nonmuscle cells.

In the following experiments we analyze the earliest stages in the nucleation of myofibrils by using antibodies against vinculin, talin, and integrin, antibodies against a battery of myofibrillar proteins as well as antibodies against nonsarcomeric contractile proteins, including caldesmon. These findings present further evidence for the proposition that the assembly of stress fibers and/or microfilament bundles in nonmuscle cells and the assembly of myofibrils in cardiac cells, although involving different proteins, share several conserved mechanisms. In addition, they also suggest that (a) cardiac myocytes are one of the few cell types that lack detectable cytoskeletal structures assembled from γ-actin, non-s-α-actinin, and caldesmon; and (b) the role of s-α-actinin in the assembly of 1.0-μm-long polarized α-actin filaments for myofibrils in muscle cells is probably similar to the role of non-s-α-actinin in the assembly of β- and γ-actin into filaments for stress fibers in fibroblasts.

Materials and Methods

Cell Culture

Chick cardiac cultures were prepared from 7-d embryos as described (21, 54). The trypsin-dissociated cells were grown on glass coverslips at a density of one heart per 35-mm tissue culture dish in a humidified 5% CO_2 incubator. The day after plating, nutrient medium was replaced with growth medium (5% FCS, 50 U/ml penicillin, 50 μg/ml streptomycin in MEM). Elimination of glutamine from the medium has been shown to facilitate the culture of cardiac myocytes by greatly reducing the proliferation of cardiac fibroblasts. Growth medium was replaced every day. Most observations were made on 5–7-d cultures. Dermal fibroblast cultures were prepared by removing the dermis from the skin of 11-d chick embryos, mincing it, and placing in CalMg-free saline (CMF) containing 0.25% trypsin for 30 min at 37°C. Cultures were passaged 4–5 times to remove any contaminating muscle. Confluent cultures were used for Northern blots.

Antibodies

Unless stated otherwise, each polyclonal and monoclonal antibody used in this study has been shown to be specific for its respective antigen, both by immunocytochemistry and immunoblots. The polyclonal anti-desmin has been described; it does not stain vimentin either in cells or blots (7). Three antibodies to α-actinin are used. Two are specific for muscle α-actinin, a mAb (9A2B8) (54), and an affinity-purified polyclonal antibody (22). Both recognize α-actinin in cardiac and skeletal myogenic cells, but do not stain stress fibers or APs in cultured chick muscle fibroblasts, pigmented epithelial cells, or PTK2 cells. These antibodies are used interchangeably and are

referred to as "anti-s-α-actinin". A polyclonal antibody against α-actinin purchased from Sigma Chemical Co. (St. Louis, MO) intensely stains both stress fibers and APs in nonmuscle cells. It does not stain Z-bands, the α-actin/s-α-actinin/troponin complexes (see below), or SAPs in myocytes packed with mature myofibrils. However, this antibody occasionally cross reacts weakly with these muscle structures in myocytes with nascent myofibrils. The basis for this weak cross-reaction is being investigated. This antibody is referred to as "anti-non-s-α-actinin". The antibody against chicken gizzard vinculin, VIN-11-5, a mouse mAb (Sigma Chemical Co.), specifically stains APs of cultured cells. Rabbit anti-talin, an affinity-purified antibody, is a gift of Dr. K. Burridge (University of North Carolina, Chapel Hill, NC). This antibody stains APs and ruffled membranes of cultured fibroblasts (11). A mouse mAb, mAb B4, is a gift of Dr. J. L. Lessard (University of Cincinnati, Cincinnati, OH). This antibody recognizes all α-actin isoforms in immunoblots and in immunofluorescence microscopy (40). A rabbit polyclonal antiskeletal troponin is a gift from Dr. S. Hitchcock-DeGregori (Robert Wood Johnson Medical School, Piscataway, NJ). In immunoblots at the concentration used (1:3,000), this antibody binds to troponin-I but not troponin-T or -C. This antibody stains I-bands in cultured skeletal myotubes and cardiac myocytes (54). Monoclonal anti-titin T20 and T30 are gifts from Dr. K. Weber, Max Planck Institute (Goettingen). These two antibodies recognize epitopes at the Z-line and A-band, respectively, in striated skeletal and cardiac muscles (25, 54). Monoclonal anti-sarcomeric myosin heavy chain (MHC) (F4G3), a gift from Dr. F. Pepe (University of Pennsylvania, Philadelphia, PA), recognizes MHC from cardiac and skeletal muscle cells only (41, 42). Affinity-purified polyclonal anti-desmoplakin is a gift from Dr. J. Nelson (Stanford University, Stanford, CA) and intensely stains desmosomes in MDCK cells (49). Anti-γ-actin, a gift from Dr. C. Bulinski (Columbia University, New York) stains stress fibers in a variety of cell types (45). mAb to A-CAM (Sigma Chemical Co.) stains intercellular junctions formed by epithelial cells in culture, using indirect immunofluorescence. Polyclonal anti-caldesmon, a gift from Dr. J. Bryan (Baylor College of Medicine, Houston, TX), stains stress fibers in nonmuscle cells (9, 20). Polyclonal anti-integrin, a gift from C. Buck (Wistar Institute, Philadelphia, PA), stains APs of fibroblasts. Polyclonal anti-non-s-MHC (Biomedical Technologies Inc., Stroughton, MA) stains stress fibers in fibroblasts but does not decorate A-bands in myofibrils.

Immunofluorescence Staining and Microscopy

For immunofluorescence microscopy cultures were rinsed with PBS and fixed with 2% formaldehyde in PBS for 3 min at room temperature. They were then permeabilized with 0.5% Triton-X 100 (Sigma Chemical Co.) in PBS for 30 min. This PBS–Triton solution was also used for all subsequent antibody washing steps. For staining with mAb B4, cells were fixed for 5 min in cold (−20°C) methanol. All primary antibodies were used at appropriate dilution for 1 h and washed three times for 10 min each. All secondary goat antibodies (Jackson ImmunoResearch Laboratories, West Grove, PA) were affinity purified and tagged with either rhodamine, Texas red, or fluorescein and used at 1:250 dilution. Some dishes were stained with p-phalloidin (3.3 μM, Molecular Probes, Inc., Eugene, OR) which was used at 1:100 in 1 ml of PBS for 20 min. Each series of experiments was performed in duplicate and included reciprocal staining. The nuclear dye, DAPI (4, 6-Diamidino-2-phenylindole dihydrochloride, Polysciences) was used at 0.2 mg/ml in 0.9% NaCl for 5 min. Specimens were mounted in 60% glycerol in PBS containing 2.5% DABCO (1, 4-diazabicyclo [2,2,2] octane; Sigma Chemical Co.). Cells were examined with an epifluorescence microscope (Carl Zeiss, Inc., Thornwood, NY), using filter sets which were selective for rhodamine, fluorescein, or the blue wavelength channel. Photographs were taken on 400 ASA film (TMAX; Eastman Kodak Co., Rochester, NY).

A laser scanning confocal microscope (model MRC 600; BioRad Laboratories, Cambridge, MA) was used for optical sectioning of double-labeled cultured cardiac myocytes. Double labeling was done with fluorescein and either rhodamine- or Texas red–conjugated secondaries or fluorescein-conjugated secondaries and rhodamine phalloidin. Efficient separation of the various fluorochromes between the two channels was achieved with the use of the 476- and 568-nm lines from a Krypton laser and a set of filters (Omega Optical Inc., Brattleboro, VT) stringently designed for this purpose. Scanning was done with a 60× planapo lens having a numerical aperture of 1.4. This would give an optimal resolution (full width at half-maximal of the point spread function) in the Z axis of 0.7 μm using a closed pinhole in each channel of detection. However, sections were acquired with the pinhole 1/8 to 1/4 open. These sections are slightly thicker than 0.7 μm in the Z axis. Serial sections were collected using a stepping motor. Final images are projections of 8–10 serial sections and color coded.

Northern Blot Analysis

Total RNA was isolated from day seven cardiac cultures and from day five cultures of cardiac fibroblasts as described by Kratwetz et al. (38). Hybridization was performed as detailed in Choi et al. (13). The following three cDNAs were used: cardiac α-actin, 3' untranslated region generated by an Ava II digest of full length cDNA (C α-actin) (22); β-actin, 3' untranslated region (β-actin) (16); γ-actin, 3' untranslated region (γ-actin) (16).

Results

Formation of AJs in Cultured Cardiac Myocytes

During the first few days in culture the trypsinized myocytes resorb many of the myofibrils that had been assembled in the embryo, and concomitantly initiate the assembly of a new population of myofibrils. De novo assembly of myofibrils begins in day 2–4 cultures and correlates with the attachment and spreading of the cells on the substrate (for details see 42, 54). Throughout the culture period, 60–80% of the cells are readily identified as myocytes as they bind antibodies to s-α-actinin, α-actin, titin, troponin-I, and s-MHC, as well as to desmin. Cells that bind any one of the myofibrillar antibodies bind all the others. Cells that do not bind any myofibrillar antibodies, or anti-desmin, are grouped together as fibroblastic cells; they display robust ρ-phalloidin–positive stress fibers that invariably costain with antibodies to γ-actin, non-s-α-actinin, non-s-MHC, and caldesmon (see below).

Fig. 1, A–H illustrate the variation in spatial distribution and degree of maturation of myofibrillar structures in different myocytes in day 7–8 cultures. In some cells the majority of myofibrils are striated (Fig. 1, A and F); in others there is a mix of striated and nonstriated (Fig. 1, C and D). Many of the originally isolated myocytes that have contacted neighboring myocytes reconstitute typically convoluted intercalated discs. Both anti-vinculin (Fig. 1, B, E, and G) and anti-desmoplakin (Fig. 1 H), a marker for desmosomes, stain patches along the intercalated discs. These patches complement one another spatially rather than costaining identical domains (Fig. 1, G and H), a condition observed during normal in vivo development (13, 32). The reconstituted intercalated discs stain continuously with anti-A-CAM (data not shown). Examination of the intercalated discs under the confocal microscope reveals that they are displaced upwards 2–6 μm from the ventral surface of the spread cells.

Each striated myofibril in Fig. 1, A–H forms a complex plaque where its distal tip inserts into an AJ of the intercalated disc. These stain prominently with antibodies to vinculin, s-α-actinin, α-actin (not shown), troponin-I, titin, and s-MHC. They do not stain with antibodies to γ-actin, non-s-α-actinin, non-s-MHC, or caldesmon. The opposed membranes of the intercalated disc show up as negative images, or nonstaining gaps, after decoration with antibodies to vinculin and the myofibrillar proteins. No gap is observed after staining with antibodies A-CAM, or desmoplakin (Fig. 1 H). These fluorescent images are in good accord with immunoelectron studies on the mature heart; namely that the terminal s-α-actinin Z-band of the most distal sarcomere of each myofibril merges with a vinculin-positive plaque on the cytoplasmic face of the intercalated disc (60). These terminal Z-bands will be referred to as asymmetric Z-bands in that while the proximal face receives the barbed ends of polarized 1.0-μm-long thin filaments (33), the distal face of that Z-band

complexes with membrane-bound vinculin. Although close apposition occurs between cardiac cells and fibroblasts, such heterotypic interfaces do not support the formation of intercalated discs. Similarly, no structure resembling either an AJ or a desmosome is observed along the ventral surface of the spread cells contacting the collagen substrate. Nevertheless, isolated cardiac cells do assemble fine desmoplakin-positive bodies (Fig. 2). Whether the desmoplakin flecks in such cells lie free in the sarcoplasm or are embedded in the ventral surface as fine hemidesmosomes could not be resolved with the fluorescence or confocal microscopes.

In summary, the culture conditions used in these experiments permit the originally dispersed myocytes to translocate, aggregate, and faithfully reconstitute intercalated discs positive for AJs and desmosomes. In contrast to the AJs in nonmuscle cells, which consist of vinculin/non-s-α-actinin/non-s-actin complexes, AJs in cardiac myocytes consist of vinculin/s-α-actinin/α-actin complexes. Furthermore, whereas in nonmuscle cells the AJs serve as insertion sites for stress fibers and/or microfilament bundles, in cardiac myocytes they serve as insertion sites for myofibrils.

Nascent Striated Myofibrils and Their Association With SAPs

As illustrated in Fig. 3, A–D, the termini of myofibrils that are still elongating and that are associated with the free amoeboid border of cardiac cells differ from those that insert into AJs of reconstituted intercalated discs. Irrespective of length, width, or orientation, the termini of these myofibrils insert into prominent, elongated, spear-tipped SAPs. These are surprisingly complex. Each costains with antibodies to the membrane-associated proteins vinculin, talin, and integrin. Each SAP also binds antibodies to the myofibrillar proteins s-α-actinin, α-actin, troponin-I, and titin. On the other hand, the localization of anti-s-MHC to each SAP is more variable. Roughly 20% may be negative and, even when present, the anti-s-MHC is often confined to the more proximal regions of the spear-shaped SAPs. Although anti-vinculin can stain striated myofibrils to varying degrees (compare Figs. 1, 3, and 4), only intermittently does it bind to costameres as defined by Pardo et al. (47). It is unlikely that costameres play an obligatory role in the assembly of normal striated myofibrils.

Fig. 3, E and F and Fig. 4, A–H, from day 4–5 cultures, illustrate stages in the assembly of myofibrils considerably earlier than those in the previous micrographs. They depict what we term SAP/myofibril nucleation centers. Not uncommonly, a single cell will display 10–20 such SAP/myofibril nucleation centers. These consist of pairs of roughly symmetrical but oppositely oriented spear-tipped SAPs. Such pairs may lack all intervening s-α-actinin Z-bands or display 1, 2--- n typical Z-bands ~0.1 μm wide. In some cells SAP/myofibril nucleation centers display a similar overall orientation as if each had responded to a common external cue (e.g., parallel lines of tension in the cell membrane; Fig. 4, A and B). In other instances, they appear to emerge and orient independently of one another (Fig. 4, C–H); not infrequently the SAPs bifurcate. Such bifurcations, followed by subsequent elongation of the interposed myofibril, probably account for the branching characteristics of myofibrils in cultured myocytes. In addition, many images are compatible
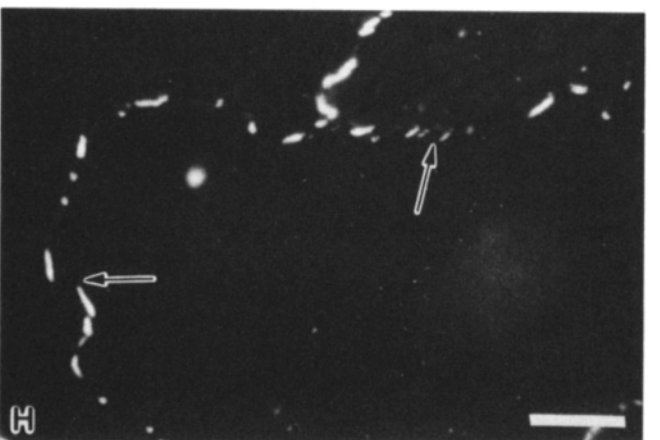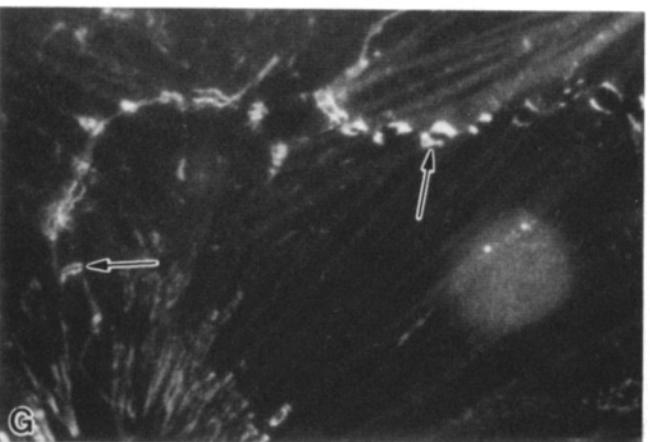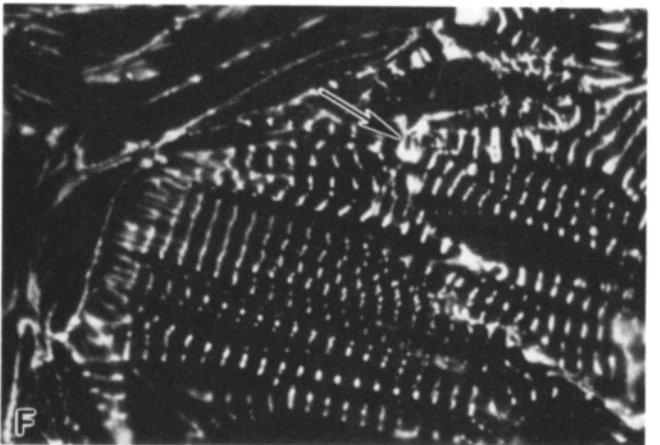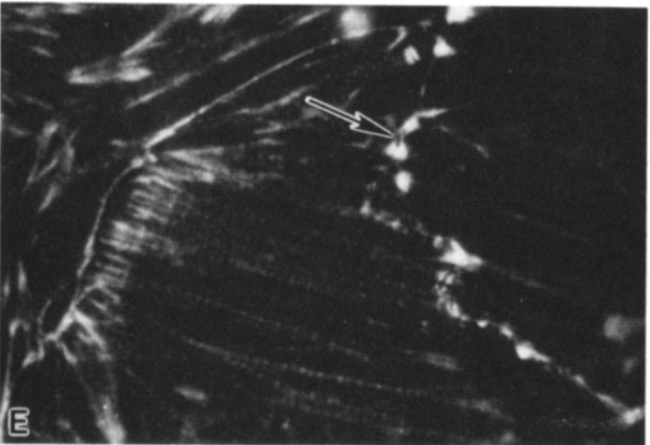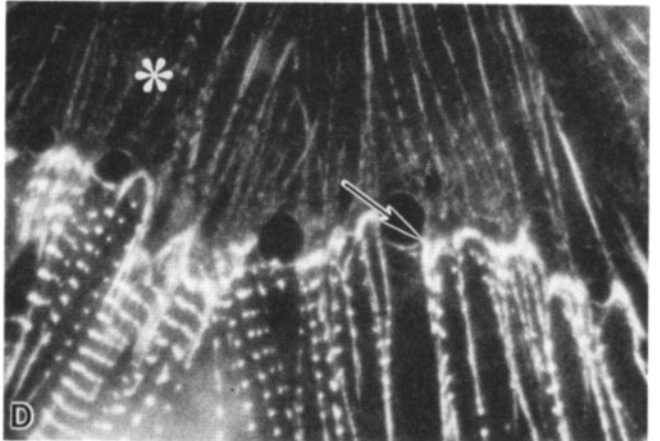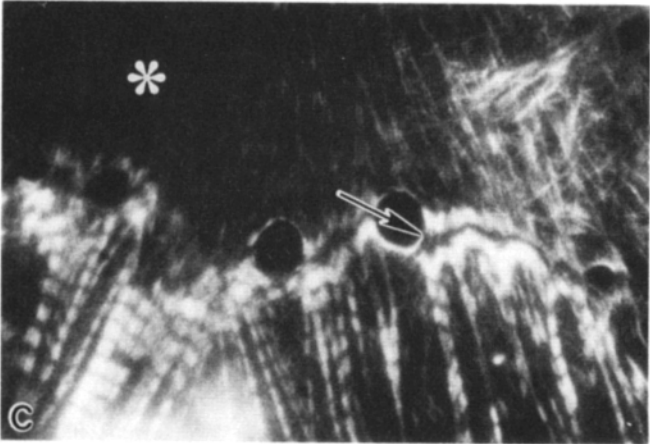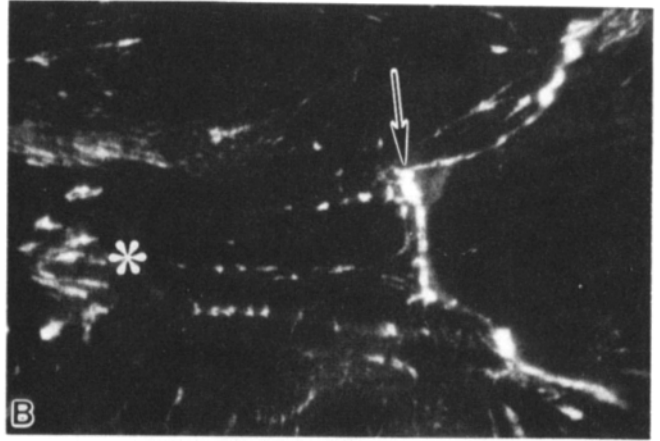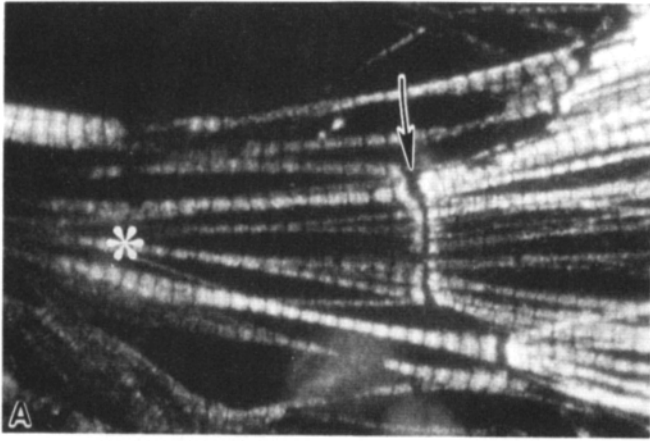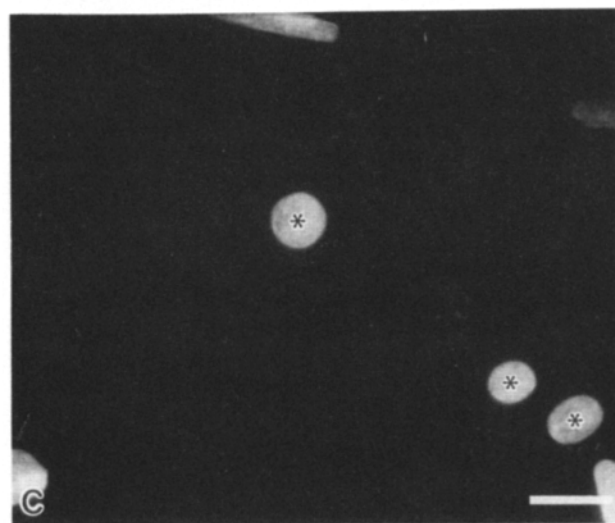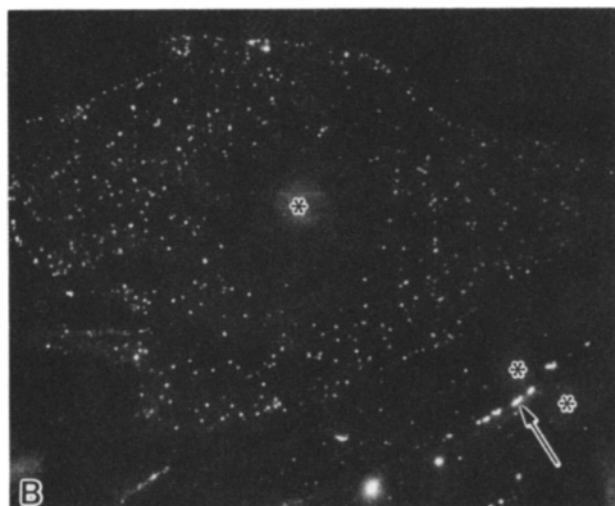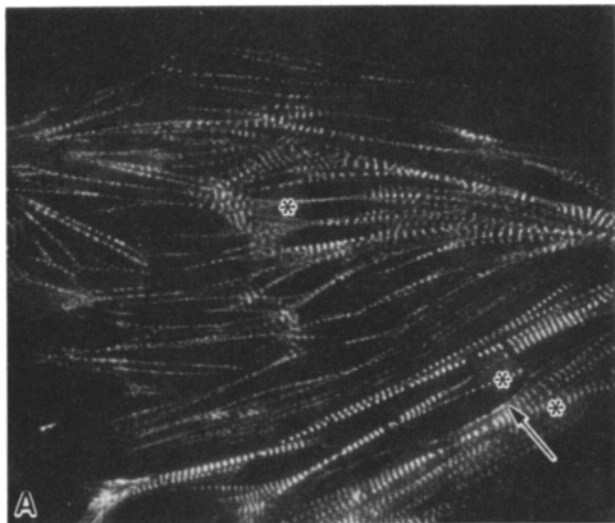
with the notion that a SAP capping one elongating nascent myofibril can fuse with a SAP from an intersecting myofibril center.

At no stage in the emergence or maturation of any SAP/myofibril center is there evidence that the prior polymerization of one myofibrillar protein acts as a template or scaffold for the others. Everywhere along the axis of a SAP/myofibril center, domains positive for troponin-I, for example, invariably are also positive for s-α-actinin, α-actin, and titin. Furthermore, the regions between each narrow s-α-actinin Z-band are without exception positive for 1.6-μm-long s-MHC-positive A-bands. MHC-positive A-bands shorter than 1.6 μm have not been observed. Efforts were made to determine whether there is a temporal sequence in the assembly of a nascent SAP. Is there a brief period when a SAP contains vinculin, α-actin, and troponin-I, for example, but lacks s-α-actinin or titin to stabilize them? As yet we have not detected a SAP lacking integrin, talin, vinculin, α-actin, α-actinin, troponin-I, or titin. Accordingly, it is likely that the assembly of a stable SAP/myofibril nucleation center requires the simultaneous interaction of at least three membrane-associated proteins and four myofibrillar proteins. If, on the other hand, the assembly of a SAP/myofibril nucleation center required but an hour or so, then such intermediate stages might have been missed given our microscopic techniques (e.g., 34).

SAPs are readily differentiated from their functional equivalents, the AJs of intercalated discs. Although both are positive for a vinculin/s-α-actinin/α-actin linkage, every SAP also costains with talin and integrin, whereas AJs are negative for these membrane-associated proteins (Fig. 5, A–D). In contrast to AJs, SAPs are negative for A-CAM. It is to be emphasized that APs in the fibroblasts in these cultures (as in all cultured nonmuscle cells) are positive for vinculin, talin, and integrin as well as ρ-phalloidin, γ-actin and caldesmon (see below).

Through focusing with the fluorescence microscope, it is revealed that SAP/myofibril nucleation centers do not assemble along the dorsal surface of the cultured cardiac cells. SAPs, whether capping a myofibril of 1 or 100 tandem sarcomeres, are assembled and are anchored to the cell's ventral

Figure 2. A group of three myocytes in a day four culture. One spread, isolated cardiac cell is in the center and two nearby thicker cardiac cells are at the lower right. *A* is stained with anti-s-α-actinin (fluorescein) and *B* is stained with anti-desmoplakin (rhodamine). Note the wide-spread distribution of the desmoplakin-positive flecks in the isolated myocyte that has failed to reconstitute an intercalated disc. In contrast, the arrow marks the incomplete desmoplakin-positive intercalated disc between the lower two contacting thicker myocytes. The asterisks mark the nuclei of the three myocytes. Note the nuclei of the nearby fibroblasts in *C* (stained for DNA with DAPI) that are negative for s-α-actinin and desmoplakin. Bar, 10 μm.

Figure 1. Micrographs of double-stained cultures illustrating the similarities between the in vitro–reconstituted intercalated discs and their in vivo counterparts. *A* and *B* are stained with anti–troponin-I (rhodamine) and anti-vinculin (fluorescein). *C* and *D* are stained with anti–s-MHC (rhodamine) and anti-s-α-actinin (fluorescein). Compare the wide nonfluorescent gap along the intercalated discs after staining with anti–troponin-I (*arrow* in *A*) or anti–s-MHC (*arrow* in *C*) with the absence of a gap observed after staining with anti-vinculin (*arrow* in *B*) or anti–s-α-actinin (*arrow* in *D*). Note too, that the numerous fine nonstriated myofibrils revealed by anti-s-α-actinin in *D* are barely stained by anti–s-MHC in *C* (*asterisks*). *E* and *F* are stained with anti-vinculin (fluorescein) and anti-s-α-actinin (rhodamine). Domains along the plicated intercalated disc positive for vinculin (*arrow* in *E*) often are coextensive with amorphous foci of s-α-actinin (*arrow* in *F*): in vivo, the latter are called "streaming Z-bands" (24). *G* and *H* are stained with anti-vinculin (rhodamine) and anti-desmoplakin (fluorescein). The spatial distribution of the vinculin in the plane of the intercalated disc (*arrows*) complements that of the desmoplakin rather than being coextensive. Bar, 10 μm.
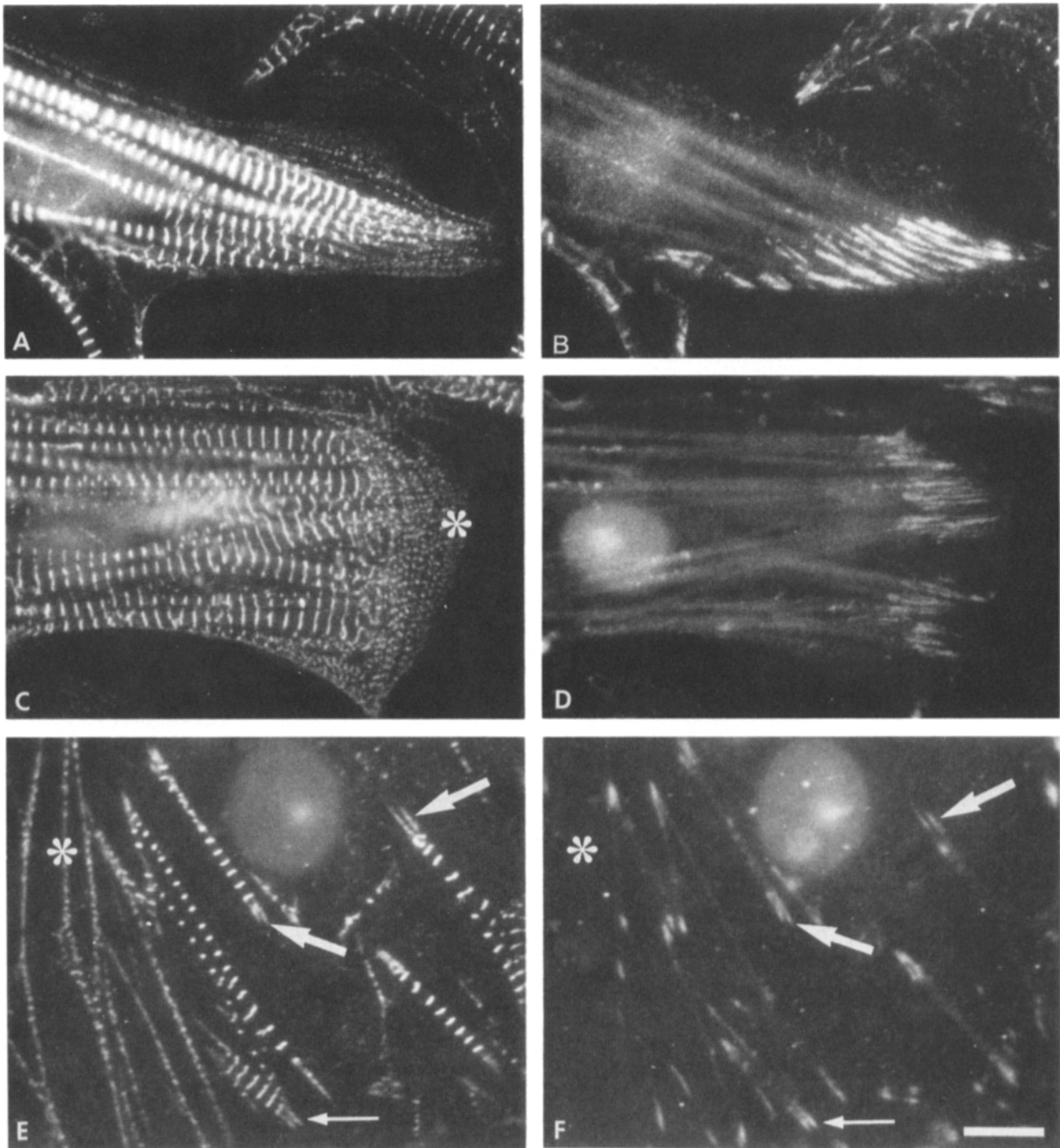
Figure 3. Micrographs of double-stained cultures illustrating changes in the SAP/myofibril complexes associated with maturation. *A–D* are of myocytes from a day eight culture and *E* and *F* from a day four culture. *A*, *C*, and *E* are stained with anti-s–α-actinin (fluorescein), *B*, *D*, and *F* with anti-vinculin (rhodamine). Both the relatively mature (*B* and *D*) and the nascent (*F*) striated myofibrils terminate in spear-tipped vinculin-positive SAPs. However, only the SAPs at the tip of the nascent myofibrils in *E* costains precisely with antibodies to s–α-actinin. Note the variable association of SAPs with the linearly aligned I-Z-I-like complexes in *E* (*asterisks*); frequently the I-Z-I-like complexes are negative for MHC fibrils (see below). The faintly fluorescent spheres are because of bleed-through of DAPI-stained nuclei. Bar, 10 μm.

Figure 4. Micrographs of double-stained myocytes from day four cultures showing early SAP/myofibril nucleation centers in single myocytes. *A* and *C* are stained with antibodies to s–α-actinin (fluorescein); *B* and *D* with antibodies to titin (rhodamine). This particular anti-titin (T20) binds to an epitope at the Z-band. Note at this early stage both the s–α-actinin and the titin are not only components of the definitive Z-bands and aligned I-Z-I-like complexes, but of the membrane-associated spear-tipped SAPs as well (*arrows*). *E* and *G* are stained with antibodies to s–α-actinin, *F* with anti-vinculin, and *H* with anti-talin. The precise costaining of s–α-actinin and titin with the membrane-associated proteins vinculin, talin, and integrin (not shown) is striking. Note the opposite polarity of the SAP at each end of a given myofibril. Asterisks and stars are for purpose of orientation. Bar, 10 μm.
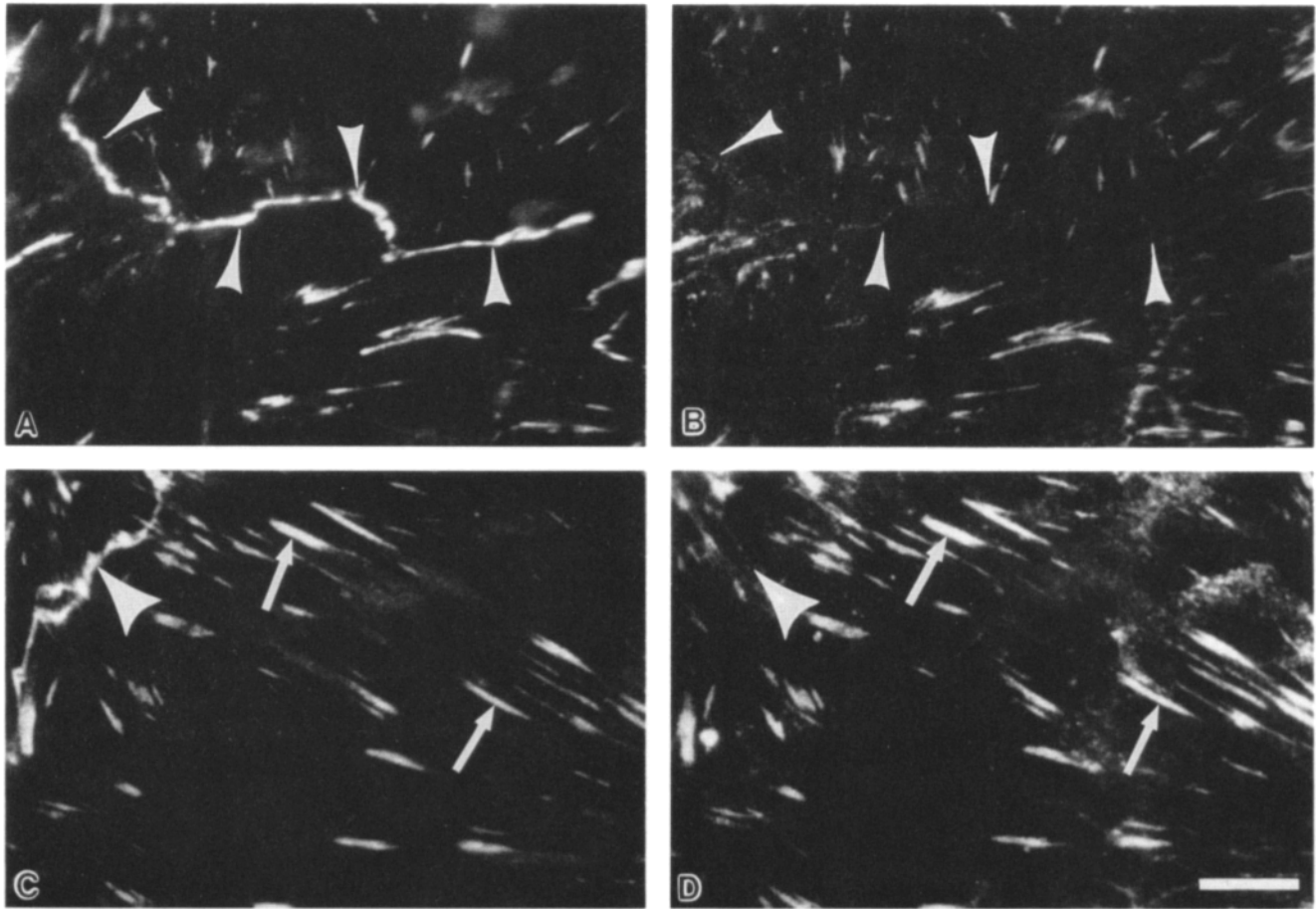
1012
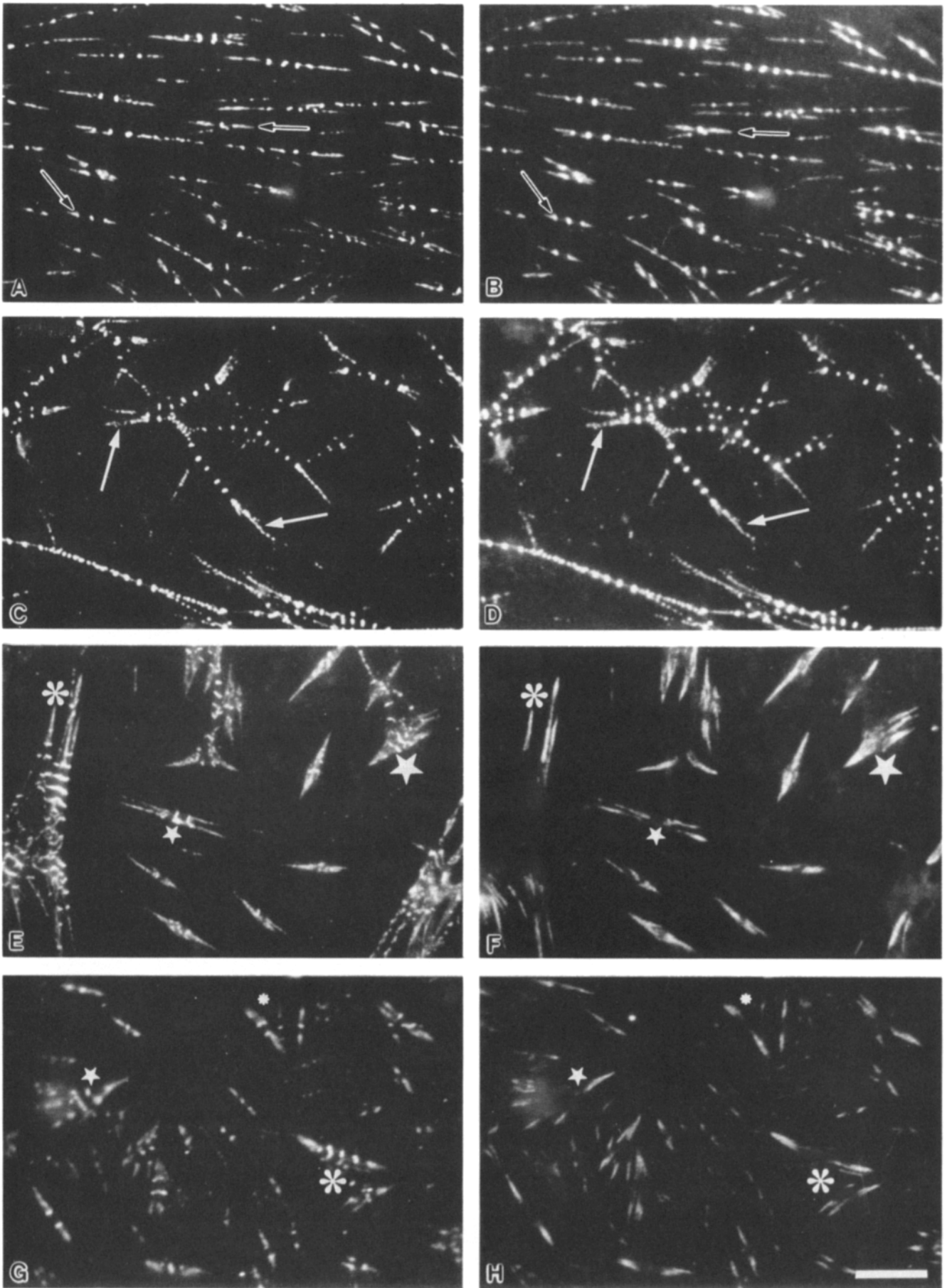
Figure 5. Double-stained cardiac myocytes from a day five culture illustrating the relationship of three different membrane-associated proteins in cardiac myocyte. *A* and *C* are stained with anti-vinculin (rhodamine), *B* with talin (fluorescein), *D* with integrin. Note the presence of vinculin (*arrowheads*) in intercalated discs but the absence of talin and integrin. Talin and integrin are excluded from cell–cell junctions, but are present in membrane-substrate junctions. Arrows point to SAPs. Bar, 10 μm.

surface only. They are not present in the region of active lammellipodia but originate many micrometers proximal to the cell's advancing growth tip.

Immunoelectron microscopic studies of intact heart, using gold-tagged antibodies, led to the conclusion that in the intercalated disc vinculin was located closer to the sarcolemma than the juxtaposed s–α-actinin of the terminal asymmetric Z-band (60). Accordingly, SAPs similar to those illustrated in Figs. 3, 4, and 5 were subject to optical sectioning with the confocal microscope. If vinculin or talin lies closer to the ventral surface than s–α-actinin and associated I-band proteins, then this distribution in the Z-axis is beyond the resolution of the confocal microscope (e.g., ∼0.7 μm). The vinculin/s–α-actinin/α-actin plaques measure 1.5–2.0 μm in thickness ($n = 6$).

In summary, the localization of SAPs to the ventral surface reveals an unsuspected dorsal–ventral polarity in cultured cardiac myocytes. For unknown reasons the in vitro ventral surface is a more favorable nucleation site for myofibrils than is the dorsal surface. Finally, while SAPs in cardiac cells and APs in nonmuscle cells assemble integrin/talin/vinculin complexes at the cell–substrate junctions, proximally they are linked to different structures, namely myofibrils and stress fibers, respectively.

Remodeling of SAPs with Maturation

There are changes in the molecular composition of SAPs as the cells mature and their myofibrils increase in sarcomere number and girth. At all stages SAPs costain with talin and integrin. But as the myofibrils cease to elongate in day eight and older cultures, the SAPs lose all myofibrillar proteins except α-actin. For example, the double-stained micrographs in Fig. 6 demonstrate that the SAPs capping mature myofibrils stain positively for vinculin (Fig. 6 *B*) and for F-actin (Fig. 6 *D*), but no longer costain appreciably with anti-s–α-actinin (Fig. 6, *B* and *C*). Comparably mature SAPs can no longer be decorated with antibodies to troponin-I, titin, or s-MHC (data not shown). This contrasts with the presence of these myofibrillar proteins in less mature SAPs (Figs. 1, 3, and 4). On the other hand, every SAP, whether associated with an immature or mature myofibril, stains with ρ-phalloidin and anti–α-actin. There are provocative differences between the terminal Z-bands at the ends of mature myofibrils that terminate in a SAP versus those associated with an AJ. As defined earlier, the latter Z-band is asymmetrical. The terminal Z-band associated with a mature SAP, however, like all the Z-bands along the body of the myofibril, is symmetrical in that actin filaments insert into both its
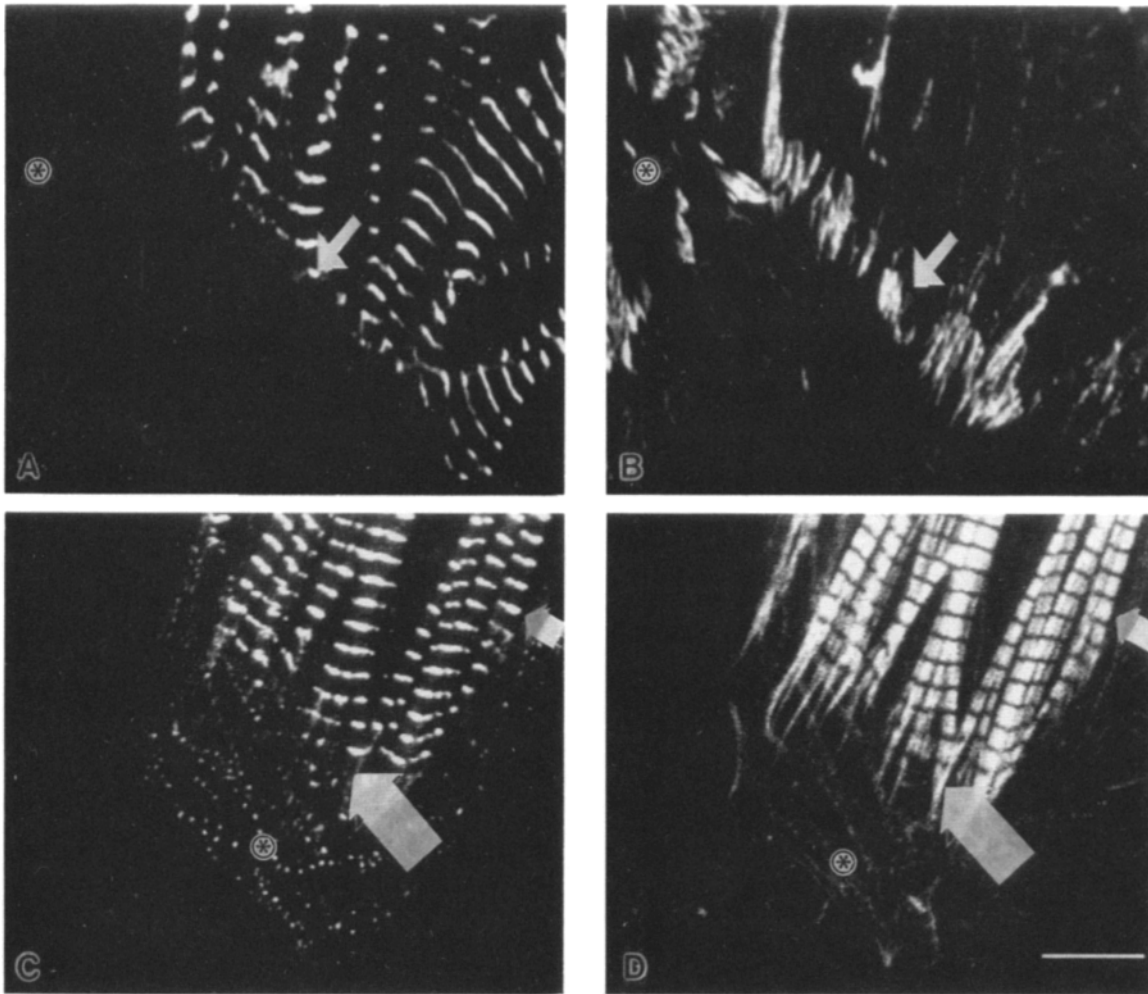
Figure 6. Confocal reconstructed images demonstrating the withdrawal of s–α-actinin, but the persistence of α-actin, in SAPs associated with mature myofibrils in day nine cultures. *A* and *C* are stained with anti-s–α-actinin (fluorescein); *B* is stained with anti-vinculin (Texas red) whereas *D* is stained with ρ-phalloidin. The absence of s–α-actinin in these SAPs contrasts with its presence in the SAPs of immature and nascent myofibrils illustrated in Figs. 3 and 4. The vinculin-positive APs of a neighboring fibroblast in *B* are indicated by an asterisk. Note the well-defined structure of each of the terminal symmetrical Z-bands. The I-Z-I-like complexes visualized with anti-s–α-actinin in *C* stain discontinuously, whereas they tend to stain continuously with ρ-phalloidin. I-Z-I-like complexes also stain continuously with anti-α-actin and anti-troponin (52). Other double-staining experiments show that all ρ-phalloidin–positive structures similar to those in *D* are positive for α-actin, but negative for γ-actin and caldesmon (see below). Direct double-staining experiments with anti-α-actin and other myofibrillar antibodies is precluded, owing to the requirement of methanol fixation when using the anti-α-actin. Bar, 10 μm.

proximal and distal faces (e.g., Fig. 6 *D*). In brief, in cultured cardiac cells one terminus of a given mature myofibril can insert into a vinculin complex at an AJ by way of its s–α-actinin positive, asymmetrical Z-band, whereas its opposite end can insert into a vinculin complex at a SAP by way of α-actin filaments from a symmetrical Z-band (compare Fig. 1, *E* and *F* with Fig. 6, *A–D*).

α-Actin/s–α-Actinin/Titin/Troponin-I Aggregates, or I-Z-I-like Complexes, and 1.6-μm-long Thick Filaments Assemble Independently of One Another and Independently of SAPs and AJs

The foregoing has focused on the termini of nascent myofibrils. However, as emphasized in earlier studies (42, 54), elsewhere in these same cells α-actin/s–α-actinin/titin/tro-

ponin-I aggregates, or I-Z-I-like complexes, as well as 1.6-μm-long MHC fibrils, are assembled. The assembly of these two classes of intermediate structures can occur independently of one another, as well as removed from either AJs or SAPs. I-Z-I-like complexes may be arranged in linear rows (*asterisks* in Figs. 3 *E*, 4 *C*, 6 *C* and see Fig. 9 *C*) or in flat patches (Figs. 3 *C* and 7 *A*); both are associated with the ventral, never the dorsal, surface. It is worth emphasizing that every microscopic s–α-actinin aggregate in these micrographs is part of a larger complex that also stains for titin, troponin-I, and α-actin. The irregular orientation of the feathery s-MHC fibrils relative to the neighboring I-Z-I-like complexes (Fig. 7, *A* and *B*) suggests little interaction at this stage between these two subassemblies. Optical sectioning reveals that the s-MHC fibrils are frequently located more dorsally in the cell than are the I-Z-I-like complexes. Al-
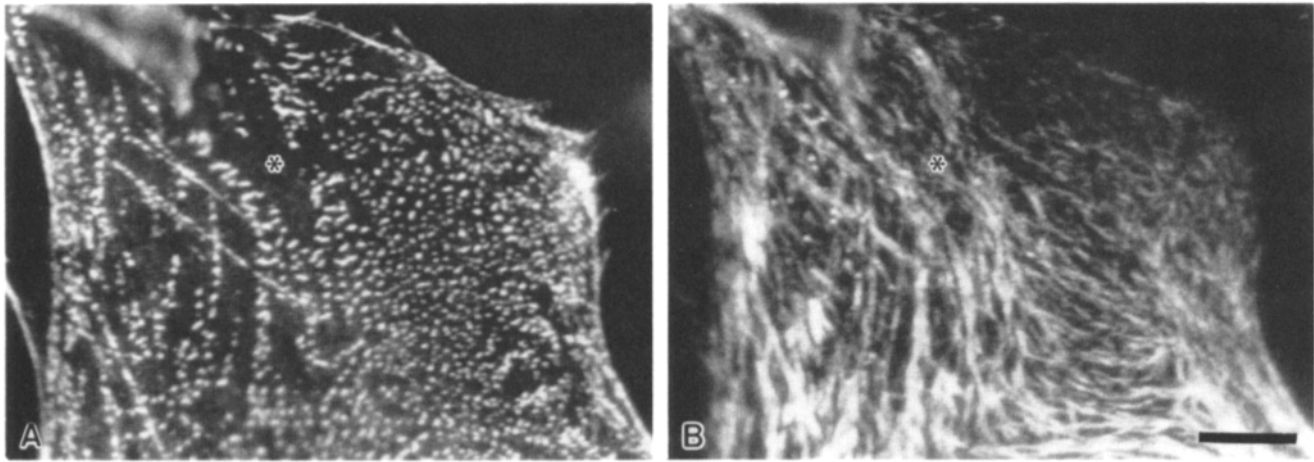
Figure 7. Day five cardiac myocyte double-stained with anti-s–α-actinin (*A*; fluorescein) and anti-s-MHC (*B*; rhodamine). The two major configurations of the I-Z-I–like complexes are illustrated in Fig. 5 A. To the left of the asterisk the I-Z-I–like complexes tend to be aligned in long strings, to the right they are deployed in an ectopic patch. The MHC-fibrils are loosely oriented with respect to the I-Z-I–like strings, whereas their orientation over the ectopic patch is irregular and independent of the precise distribution of the s–α-actinin aggregates. Vinculin/talin/integrin-positive SAPs would not be present in this region. Bar, 10 µm.

though occasionally associated with the linearly aligned complexes, SAPs are never observed in the vicinity of the I-Z-I patches (Fig. 7 *A*). It is also to be emphasized that the packaging of the s–α-actinin within the I-Z-I–like complexes is readily distinguishable from the morphology of the s–α-actinin when packaged into definitive, 0.1-µm-wide Z-bands (compare Fig. 7 *A* with Fig. 3 *E* and Fig. 4, *A–G*).

Patches of I-Z-I–like complexes and clusters of 1.6-µm-long MHC fibrils are also observed in the vicinity of intercalated discs. However, owing to the thickness of the cells in this area and the convoluted nature of the opposed cell membranes, details on the spatial relationship among these subassemblies, nascent myofibrils, and AJs tend to be obscured.

In summary, two relatively independent foci exist for the assembly of intermediate myofibrillar structures, the I-Z-I–like complexes and the 1.6-µm-long s-MHC fibrils. Both can emerge independently of SAPs and AJs. The tight linkage between a SAP, or an AJ, and the myofibrillar subassemblies seems to be limited to the immediate vicinity where the two types of intermediate structures are involved in the process of interdigitating to form a nascent sarcomere. Obviously, additional experiments are required to prove or disprove this impression.

Non-s–α-Actinin Structures Are Not Evident at Any Stage in Cardiac Myocytes

Next we asked whether at any time cardiac cells would assemble SAPs similar to those in nonmuscle cells and stain, not for s–α-actinin, but for non-s–α-actinin? Would s–α-actinin spear-shaped structures ever assemble in the plane of the sarcolemma without being linked distally to vinculin/talin/integrin plaques or without being linked proximally with such myofibrillar proteins as α-actin, titin, or troponin-I? To address these questions we used a polyclonal affinity-purified anti-s–α-actinin for two reasons: This antibody (*a*) does not decorate any structure in nonmuscle cells (see Figs. in Schultheiss et al. [54]) and (*b*) can be used in double-staining experiments with other antibodies and with ρ-phalloidin. As

shown in Fig. 8, *A* and *C* definitive Z-bands and aligned I-Z-I–like aggregates stained intensely with this anti-s–α-actinin. In contrast, the anti-non-s–α-actinin stained the fibroblast stress fibers, APs, and lamellipodia, but failed to stain the myocyte SAPs, I-Z-I–like complexes, or Z-bands (Fig. 8, *B* and *D*). It is worth emphasizing that even the α-actinin molecules constituting the immature, linearly aligned I-Z-I–like complexes are composed of the sarcomeric rather than the non-sarcomeric isoforms (Fig. 8 *C*). The AJs of the intercalated discs invariably are negative for the non-s–α-actinin. It is also evident from Fig. 8, *C–D* that while the anti–non-s–α-actinin stains the lamellipodia of translocating fibroblasts it does not stain the homologous structure of cardiac myocytes. If at any stage during the maturation of cardiac myocytes there is a switch from non-s–α-actinin to s–α-actinin either in AJs, SAPs, I-Z-I–like complexes, or Z-bands, then such a switch escaped our detection.

Since no structure in cardiac cells unequivocally stains for non-s–α-actinin, one must question whether these cells typically synthesize any non-s–α-actinin.

Stress Fiber-like Structures in Cardiac Cells Are Assembled From Sarcomeric Isoforms Only

Cardiac cells at all stages of maturation display long ρ-phalloidin bundles that are indistinguishable morphologically from stress fibers in nonmuscle cells. These bundles have been referred to as "stress fiber–like structures" or SFLS (2, 21, 29). However, our finding that no AJ or SAP was positive for non-s–α-actinin prompted us to ask whether in fact cardiac cells assemble: (*a*) authentic stress fibers (e.g., bundles of microfilaments negative for sarcomeric, but positive for non-sarcomeric proteins, including caldesmon); (*b*) hybrid structures assembled from both sarcomeric and non-sarcomeric proteins; or (*c*) stress fiber–like structures consisting exclusively of sarcomeric proteins. To distinguish among these three possibilities cultures were stained in one of two ways: (*a*) with ρ-phalloidin and an antibody to a non-sarcomeric protein (e.g., γ-actin, non-s–α-actinin, non-s-MHC,
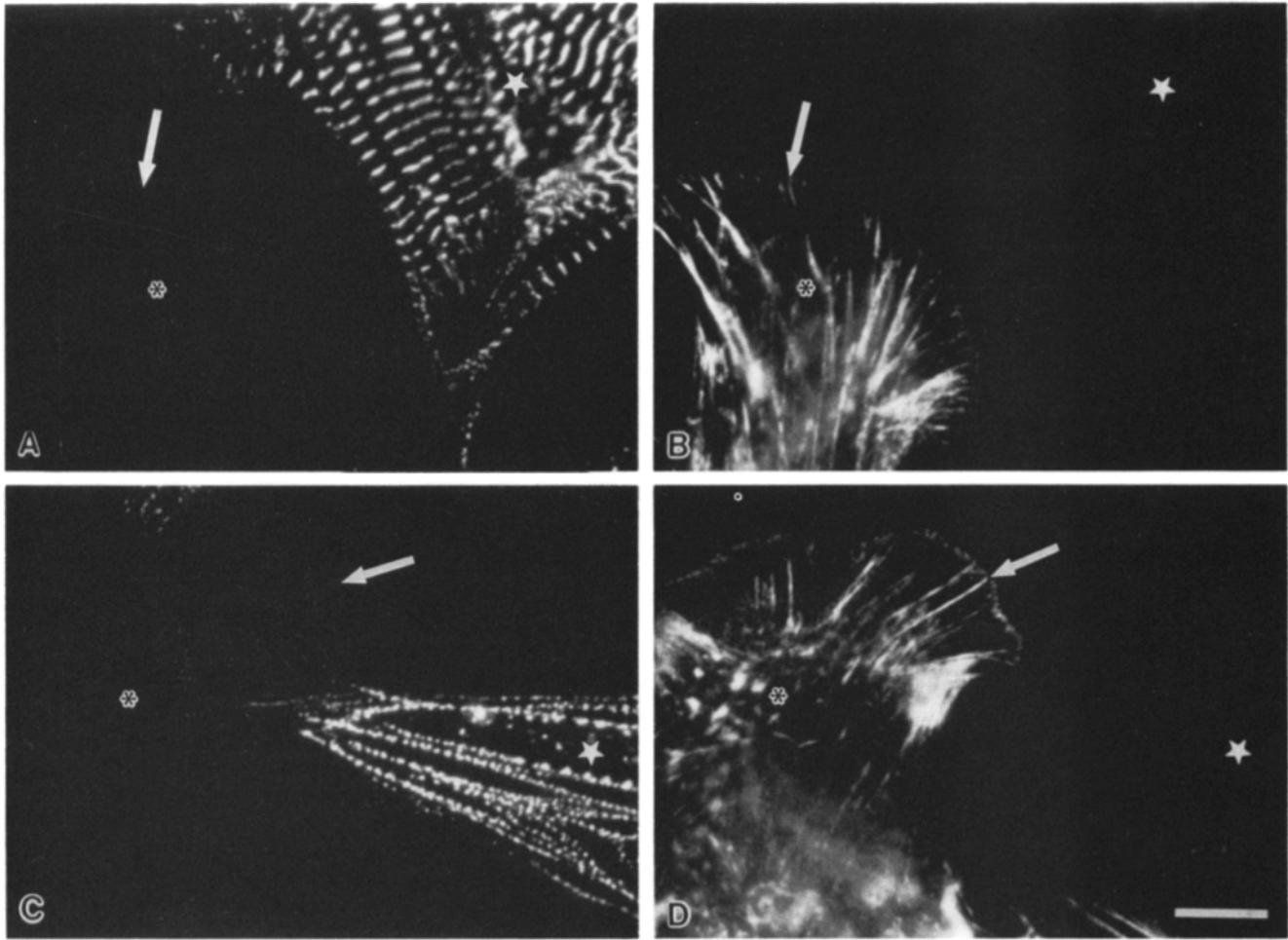
Figure 8. Double-stained micrographs to show that cardiac cells do not stain with anti–non-s–α-actinin and that fibroblasts do not stain with anti-s–α-actinin. *A* and *C* reveal the localization of anti-s–α-actinin (rhodamine), whereas *B* and *D* reveal the localization of anti–non-s–α-actinin (fluorescein). It is clear from comparing *C* and *D* that the linearly aligned I-Z-I–like complexes (presumably preassembled subunits that will be incorporated into striated myofibrils) do not contain non-s–α-actinin. *B* and *D* illustrate that although the anti–non-s–α-actinin does not stain structures in cardiac cells, in fibroblasts it stains stress fibers, APs, lamellipodia, and polygons (out of focus). Asterisks mark fibroblasts, stars mark the cardiac cells. Bar, 10 μm.

or caldesmon) or with ρ-phalloidin and an antibody to a sarcomeric protein (e.g., α-actin, s–α-actinin, troponin-I, titin, or s-MHC); and (*b*) pairwise with one antibody to a non-sarcomeric protein and another antibody to a sarcomeric protein.

Representative double-stained preparations from these experiments are illustrated in Figs. 8, 9, and 10. They demonstrate that all cardiac cells treated pairwise with one sarcomeric and one non-sarcomeric antibody are positive for the sarcomeric isoform only; cells that bind any one of the antibodies to myofibrillar proteins do not bind any antibody to the non-sarcomeric proteins, including caldesmon. Fibroblasts in these cultures are positive for caldesmon and the non-sarcomeric proteins only (Fig. 8, *A–D* and Fig. 9, *A–F*). Every ρ-phalloidin–positive structure in cardiac cells always costained with our battery of myofibrillar antibodies (Fig. 10). In no instance did ρ-phalloidin bundles in cardiac cells costain with an antibody to any non-sarcomeric protein, including caldesmon. This series of experiments also demon-

strated that, without exception, every ρ-phalloidin–positive stress fiber in fibroblasts, costained with antibodies to (*a*) non-s–α-actinin, (*b*) γ-actin, and (*c*) caldesmon. If any microscopically detectable ρ-phalloidin–positive stress fibers in fibroblasts failed to costain with antibodies to non-s–α-actinin and caldesmon, they too escaped our detection.

Data consistent with the notion that cultured cardiac cells have downregulated the synthesis of the cytoplasmic actins also derives from studies based on Northern blots. The γ-actin band from cardiac cultures is roughly 1/10 that of the equivalent band from fibroblast cultures (Fig. 11). The β-actin band from cardiac cultures is roughly 1/5 that of the fibroblast cultures. When these results are combined with the immuno-cytochemistry illustrated in Figs. 8, 9, and 10, we conclude that in all probability the bulk of the γ-actin transcripts are not in cardiac myocytes but in fibroblasts included in the analyzed population of cells. As stated earlier, 20–40% of the cells in the cardiac cultures are negative for all myofibrillar proteins, as well as for desmin. Obviously in situ
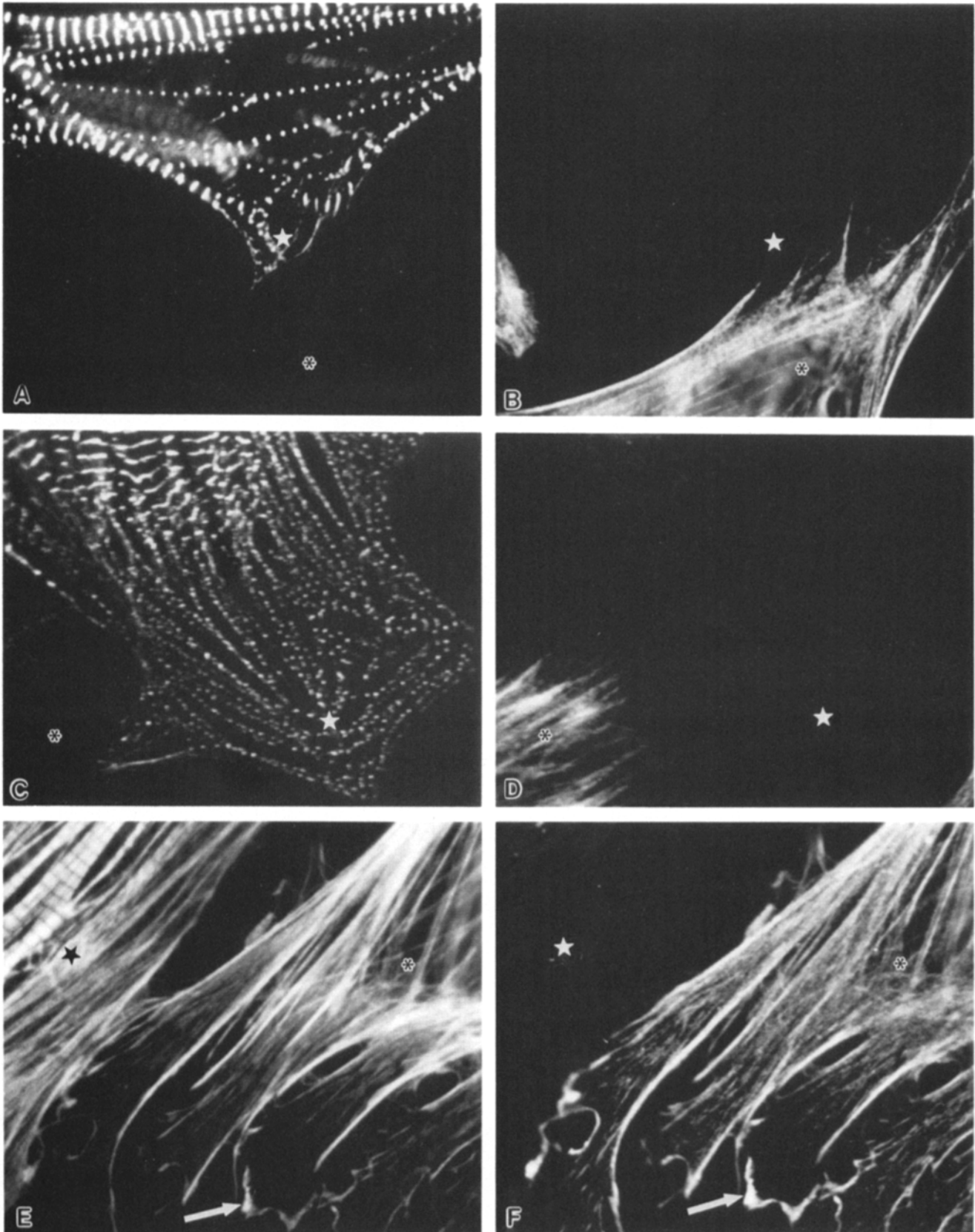
Figure 9. Micrographs of double-stained cultures demonstrate that although antibodies to non–s-MHC, γ-actin, and caldesmon stain stress fibers in fibroblasts, they do not stain any structure in cardiac cells (*asterisks* and *stars*, respectively). *A* and *B* are stained with anti-s–α-actinin (rhodamine) and anti-non–s-MHC (fluorescein). Note in *B* the periodic distribution of non–s-MHC along the axis of the stress fiber. *C* is stained with anti-s–α-actinin (fluorescein) and *D* with anti-caldesmon (rhodamine). Note the absence of caldesmon both in the linearly aligned I-Z-I-like complexes and elsewhere in the cardiac cell. The tip of a fibroblast at the lower left in *D* binds the anti-caldesmon to typical stress fibers. *E* and *F* are, respectively, stained with ρ-phalloidin to reveal all F-actin containing structures and with anti–γ-actin to reveal authentic stress fibers. In cardiac cells, ρ-phalloidin stains the definitive I-Z-I brushes of the striated myobrils, the nonstriated myofibrils or stress fiber-like structures (below the *star* in *E*), as well as the lamellipodia (not shown). *E* and *F* demonstrate that the stress fibers, AJs and lamellipodia in fibroblasts that bind ρ-phalloidin (*E*) precisely costain with anti–γ-actin (*F*; rhodamine). Note that the anti–γ-actin does not stain the stress fiber-like structures in cardiac cells. Bar, 10 μm.
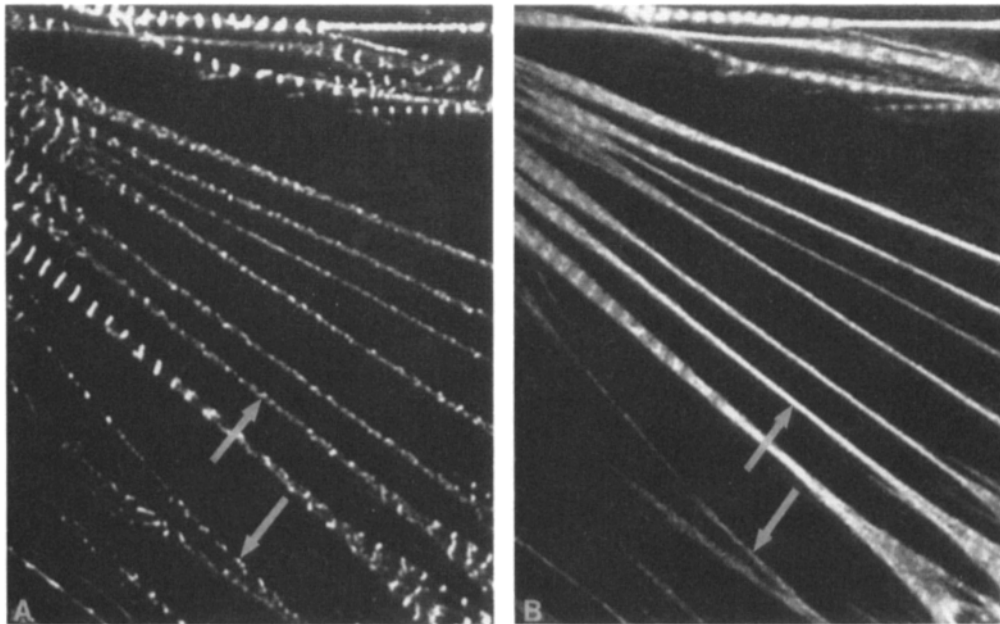
Figure 10. Micrographs of a double-stained cardiac cell illustrating that what have been termed "stress fiber–like structures" based on their appearance in ρ-phalloidin stained preparations, prove to be non-striated myofibrils consisting largely of aligned I-Z-I–like complexes. *A* reveals the localization of anti-s–α-actinin (fluorescein), whereas *B* reveals the localization of ρ-phalloidin–positive, or F-actin containing, structures. Note that the fine I-Z-I–like complexes that stain in a punctate manner with anti-s–α-actinin, stain continuously with ρ-phalloidin. Such aligned I-Z-I–like complexes also stain continuously after decoration with antibodies to α-actin, troponin-I, and titin-30.

hybridization experiments are required to resolve this issue. We have yet to determine whether anti–β-actin binds to structures in cardiac cells. Still, even if present, the level of β-actin in the myocytes is also considerably lower than in fibroblasts.

In brief, the conspicuous ρ-phalloidin–positive bundles, which in cultured myocytes have been described as stress fiber–like structures (2, 21, 29, 55), are likely to be bundles formed entirely of sarcomeric isoforms before their final remodeling into well-defined sarcomeres. When cultured cardiac cells assemble microscopically detectable F-actin bundles, they assemble α-actin destined for myofibrils, not for authentic stress fibers. Cardiac myocytes normally accumulate little, if any, γ-actin, and probably little β-actin.
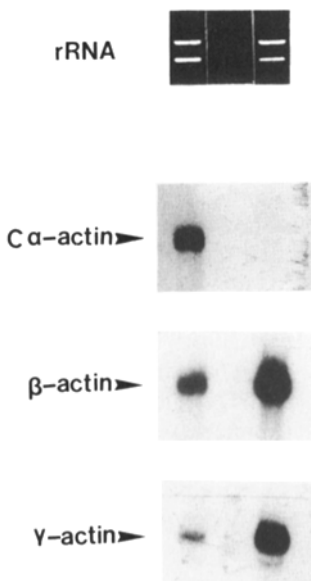

Figure 11. Northern blot analysis of day eight cardiac cultures and cultures of chick fibroblasts. 2 μg of total RNA from each culture were loaded onto each lane. *C*, cardiac culture; *F*, fibroblast culture. Blots were hybridized and stripped multiple times to generate a composite figure. Equal loading for each lane is demonstrated by ethidium bromide staining of mRNA in parallel gels.

Discussion

The conservation of AJs and APs in many cell types suggests that such complexes have been subject to strong selective pressures and that variations in their structure associated with cell diversification must be subject to developmental regulation. Furthermore, the invariant association of F-actin/α-actinin/vinculin plaques with both AJs and APs probably reflects an interdependence in assembly and/or stability, of these organelles. Not only do stress fibers terminate in APs, but it is likely that earlier in the life cycle of nonmuscle cells such complexes served another function, namely as nucleation sites for nascent, elongating stress fibers. According to Izzard and co-workers (19, 34) precursor short, rib-like actin bundles accumulate just proximal to active lamellipodia in translocating fibroblasts. Where the plasma membrane contacts the substrate, these short bundles complex, first with talin, and minutes later, with vinculin. These nascent APs stabilize and, in a manner still not understood, nucleate elongating stress fibers (27, 28, 37, 61).

The SAP/myofibril nucleation centers illustrated in Figs. 3 and 4 fit into the general scheme of where and how stress fibers are nucleated in nonmuscle cells. If SAPs exist without attached myofibrils they must be so rare, small, transient, or metastable, as to be easily overlooked. In brief, whenever and wherever cardiac cells respond to local cell-substrate conditions by vectorially assembling a stable SAP, they will have also nucleated a SAP/myofibril nucleation center and initiated the assembly of a nascent, elongating myofibril. When nonmuscle cells respond to the same cell-substrate signals by vectorially assembling a stable AP, they will have also nucleated an AP/stress fiber center and initiated the assembly of a nascent, elongating stress fiber.

AJs and SAPs appear to be equally capable of anchoring myofibrils to the sarcolemma. Differences between the two probably reside in their transmembrane and extracellular components. The two structures can be conceptualized as being composed of a myofibril-anchoring mechanism which

can be coupled to one of two types of membrane attachment. The choice of membrane attachment is likely to be governed by external factors, such as the presence of a neighboring myocyte or of extracellular matrix molecules. Such considerations are supported by the finding that the terminal Z-band at a mature SAP is symmetrical rather than asymmetrical, as it is at an immature SAP or at an AJ. The symmetrical terminal Z-band at each mature SAP is in fact characteristic of the myotendenous junction at the ends of mature skeletal muscle fibers in vivo (56).

In nonmuscle cells most α-actinin is localized to periodically distributed dense bodies which complex with F-actin along the length of the stress fiber. Interaction between non-s-α-actinin and vinculin is confined to regions where stress fibers terminate and/or originate. Similarly, in cardiac cells most s-α-actinin is packaged into repeating 0.1 μm wide, symmetrical Z-bands. Only a minute fraction of the cell's total s-α-actinin complexes with vinculin at the asymmetrical, terminal Z-band. These conserved topological relationships suggest common regulatory mechanisms for the deployment and stabilization of the involved proteins. Four observations are consistent with the proposition that conditions which stabilize or destabilize stress fibers also stabilize or destabilize myofibrils: (a) transfection of Cos cells with vinculin cDNAs lacking the talin binding regions results in resorption of both APs and attached stress fibers (6, 36); (b) mutations in the nematode vinculin gene, deb-1, results in disorganized body-wall muscles (3); (c) fibroblasts microinjected with a fragment of non-s-α-actinin lacking the β-integrin binding site, resorb their APs and attached stress fibers (50); and (d) PTK2 cells transfected with a truncated s-α-actinin cDNA lacking EF hands, resorb their APs and attached stress fibers, whereas similarly transfected myotubes resorb their SAPs and attached myofibrils[2] (our own unpublished data).

One of the earliest reports suggesting that all cells synthesize and accumulate sizeable quantities of actin monomers derives from morphological studies using heavy meromyosin to decorate cultured muscle cells (33). What remains unresolved is whether the isoform type(s) comprising the monomer pool is largely α-, β-, or γ-actin. All studies agree that the cytoplasmic actin mRNAs are downregulated to unknown degrees during muscle maturation (22, 30, 52). On the other hand, studies examining the cytoplasmic actins in developing muscle are contradictory. Lubit and Schwartz (43) report that an antibody against Aplasia actin stained the sarcolemma of cultured myotubes but not their myofibrils or mitochondria. Pardo et al. (48) state that an affinity-purified anti-γ-actin did not stain myofibrils, but stained mitochondria. Otey et al. (45) report that their anti-γ-actin stained microfilament bundles in L6 myotubes, but did not stain mitochondria. Rubinstein et al. (51) and Denning et al. (18), using biochemical and cyto-immunofluorescent techniques, respectively, concluded that β- and γ-actin is selectively eliminated from cultured myotubes in small bodies termed macules. Lin et al. (41, 42), however, contend that both normal and TPA-treated myotubes selectively eliminate their muscle specific I-Z-I proteins by packing them into 3.0-μm bodies surrounded by vinculin/talin/integrin rims.

The data in this report introduce still other considerations regarding the synthesis and targeting of non-sarcomeric proteins in cardiac cells. The most straightforward interpretation of our findings is that relatively mature myocytes, in contrast to most nonmuscle cells, do not normally assemble stress fibers consisting of γ-actin, non-s-α-actinin, non-s-MHC, and caldesmon. Differences in interpretation of our current findings compared with previous studies of ours and those of others are not likely to be explained on the basis that our antibodies are less specific, have lower titers, bind to fewer and/or less accessible epitopes, etc. Such explanations can not account for the simple observation that authentic stress fibers (ρ-phalloidin–positive structures that costain with antibodies to non-sarcomeric contractile proteins) are not observed in cultured cardiac cells. In addition, faint and/or inconstant staining, particularly with different anti-actins or different batches of anti-non-s-actinin, is difficult to interpret unequivocally (e.g., compare Figs. of Handel et al. [29] and Pardo et al. [48] with those in this report). Accordingly, it is appropriate to raise the question of what combinations of contractile proteins in cardiac cells mediate the myriad functions performed by non-sarcomeric contractile proteins in nonmuscle cells. In cardiac cells, are ruffled membrane formation, migration, pinocytosis, regulation of distribution of integral membrane proteins, etc., controlled by structures assembled from sarcomeric isoforms? In cardiac cells, can such functions be mediated in the absence of caldesmon?

One of our long term goals is to relate the properties of the contractile protein isoforms, as determined in cell-free systems, to their behavior in living cells. For example, in solution antipolar homodimers of s-α-actinin self-aggregate and cross-link F-actin; whereas they do not bind G-actin, nor nucleate actin polymerization (8). In cardiac cells the finest microscopic aggregates localized with anti-s-α-actinin appear as part of larger complexes which also stain with ρ-phalloidin and with antibodies to α-actin, troponin-I, and titin. Similar sized non-s-α-actinin aggregates in fibroblasts also are parts of larger complexes that stain with ρ-phalloidin, but in these cells the complexes are also positive for γ-actin and caldesmon. Recent observations made on PTK2 and muscle cells transfected with s-α-actinin cDNAs are also consistent with the notion that in vivo nascent s-α-actinin molecules are more likely to assemble rapidly and selectively into structures with other contractile proteins rather than to undergo exclusive self-aggregation into microscopically detectable structures. Choi et al.[2] report that the earliest expression of exogenous s-α-actinin in transfected PTK2 cells is not in microscopic aggregates of s-α-actinin alone, but is localized in beaded dense bodies incorporated into stress fibers which stain with ρ-phalloidin as well as with antibodies to γ-actin, non-s-α-actinin, and caldesmon. In transfected muscle cells, the earliest expressed exogenous s-α-actinin is found in structures that stain with ρ-phalloidin and antibodies to α-actin, troponin-I, and titin. In brief, in both normal and transfected nonmuscle and muscle cells, the assembly of α-actinin-containing structures is linked with some actin isoform together with other contractile proteins. Similarly, the actins destined for stress fibers in nonmuscle cells and the α-actin destined for thin filaments in myofibrils invariably are linked to the appropriate α-acti-

---

2. Choi, J., T. Schultheiss, Z. Lin, and H. Holtzer. 1991. *J. Cell Biol.* 115: 964 (Abstr.).

nin isoform together with other appropriate contractile proteins. These observations raise the question of the minimal number of contractile proteins required in vivo for assembling (a) morphologically recognizable stress fibers or striated myofibrils, or (b) I-Z-I-like complexes and 1.6-μm-long, bipolar, tapered thick filaments.

The term "stress fiber–like structures", or SFLSs, was coined to describe the transient nonstriated myofibrils that often precede the appearance of striated myofibrils in immature myogenic cells. These may be positive for both sarcomeric and non-sarcomeric proteins (2, 21). This formulation left unresolved whether SFLSs consist of chimeric filaments (e.g., heteropolymers of α-, β-, and γ-actins, s-MHC and non–s-MHC, etc.), or how with time the sarcomeric proteins sorted out into invariant, tandem sarcomeres. While the data in this report do not resolve these issues, they are germane to the proposal that the transition from nonstriated to striated myofibrils reflects the monotonic lengthening of tandem "mini-sarcomeres". Mini-sarcomeres have been defined by Sanger et al. (53) as strings of definitive Z-bands with periodicities varying progressively from $\pm$ 0.6 μm to the mature periodicity of $\pm$ 2.0 μm. As the distance between Z-bands increases the short, laterally aligned, interposed thick filaments are claimed to lengthen proportionately. The fine structure, molecular composition, and relatively independent distribution and assembly of the I-Z-I-like complexes and the 1.6-μm-long MHC-thick filaments described in this paper (see also 54) are all incompatible with the notion that mini-sarcomeres gradually transform into striated myofibrils.

Definitively striated myofibrils positive for s–α-actinin, titin, MHC, and troponin-I first appear in replicating $\pm$ stage 9 cardiac cells and in postmitotic $\pm$ stage 15 somitic mononucleated myoblasts (13, 31, 32). Similarly striated cardiac and skeletal myogenic cells emerge in cultures prepared from dissociated $\pm$ stage 4 blastula cells that terminally differentiate in the absence of recognizable entoderm and neural tissue. It will be interesting to determine the status of the α-actinin isoforms in these early mitotically active and inactive muscle cells.

Our findings lead us to postulate that s–α-actinin plays a direct role in the assembly of I-Z-I-like complexes, but only an indirect one in the assembly of tandem sarcomeres. This finding is consistent with the observation that skeletal myoblasts reared in taxol, in addition to assembling long microtubules, assemble 1.6-μm-long bipolar thick filaments that align laterally into "pseudostriated" myofibrils in the total absence of I-Z-I structures (1, 57). Still the notion that in muscle cells s–α-actinin, together with other I-Z-I proteins, is essential for the assembly and/or stabilizaton of SAPs and Z-bands, or that in fibroblasts non-s–α-actinin is essential for the assembly and/or stabilization of APs and dense bodies, should be viewed in the context of gene disruption experiments in Dictyostelium. Mutants in these cells lacking α-actinin do not display gross changes in motility, phagocytosis, or chemotaxis. These cells, however, do not assemble APs, AJs, or stress fibers. This may mean that over the course of evolution α-actinin has changed its functions. To determine whether there is an obligatory requirement for α-actinin, either for the initiation, or the stabilization, of SAPs and APs, or Z-bands and dense bodies, null mutants must be generated in muscle and nonmuscle cells in higher forms.

References

1. Antin, P., S. Forry-Schaudies, S. Tapscott, and H. Holtzer. 1981. Taxol induces postmitotic myoblasts to assemble interdigitating microtubule-myosin arrays that exclude actin filaments. *J. Cell Biol.* 90:300-308.
2. Antin, P., S. Tokunaka, V. Nachmias, and H. Holtzer. 1986. Role of stress fiber-like structures in assembling nascent myofibrils in myosheets recovering from exposure to ethyl methanesulfonate. *J. Cell Biol.* 102:1464-1479.
3. Barstead, R. J., and R. H. Waterston. 1991. Vinculin is essential for muscle function in the nematode. *J. Cell Biol.* 114:715-724.
4. Beckerle, M. C., and R. K. Yeh. 1990. Talin: role at sites of cell-substratum adhesion. *Cell Motil. Cytoskeleton.* 16:7-13.
5. Beckerle, M. C., K. Burridge, G. N. DeMartino, and D. E. Croall. 1987. Colocalization of calcium-dependent protease II and one of its substrates at sites of cell adhesion. *Cell.* 51:569-577.
6. Bendori, R., D. Salomon, B. Geiger. 1989. Identification of two distinct functional domains on vinculin involved in its association with focal contacts. *J. Cell Biol.* 108:2383-2393.
7. Bennett, G. S., S. A. Fellini, and H. Holtzer. 1978. Immunofluorescent visualization of 100 A filaments in different cultured chick embryonic cell types. *Differentiation.* 12:71-82.
8. Blanchard, A., V. Ohanian, and D. Critchley. 1989. The structure and function of α-actinin. *J. Muscle Res. and Cell Motil.* 10:280-289.
9. Bretscher, A., and W. Lynch. 1985. Identification and localization of immunoreactive forms of caldesmon in smooth and nonmuscle cells: a comparison with the distributions of tropomyosin and α-actinin. *J. Cell Biol.* 100:1656-1663.
10. Burridge, K. 1986. Substrate adhesions in normal and transformed fibroblasts: organization and regulation of cytoskeletal, membrane and extracellular matrix components at focal contacts. *Cancer Rev.* 4:18-78.
11. Burridge, K., and L. Connell. 1983. A new protein of adhesion plaques and ruffling membranes. *J. Cell Biol.* 97:359-367.
12. Burridge, K., and J. R. Feramisco. 1981. Non-muscle α-actinins are calcium-sensitive actin-binding proteins. *Nature (Lond.).* 294:565-567.
13. Choi, J., T. Schultheiss, M. Lu, W. Franke, D. Bader, D. Fishman, and H. Holtzer. 1988. Founder cells for the cardiac and skeletal myogenic lineage. *In* Cellular and Molecular Biology of Muscle Development. F. Stockdale and L. Kedes, editors. Alan R. Liss, Inc., New York. 27-36.
14. Choi, J., S. Holtzer, Z. Lin, R. Hoffman, and H. Holtzer. 1991. Phorbol esters selectively and reversibly inhibit a subset of myofibrillar genes responsible for the ongoing differentiation program of chick skeletal myotubes. *Mol. Cell. Biol.* 11:4473-4482.
15. Deleted in proof.
16. Cleveland, D. W., M. A. Lopata, R. J. MacDonald, N. J. Cowan, W. J. Rutter, and M. W. Kirschner. 1980. Number and evolutionary conservation of α- and β-tubulin and cytoplasmic β- and γ-actin genes using specific cloned cDNA probes. *Cell.* 20:95-105.
17. Damsky, C. H., K. A. Knudsen, D. Bradley, C. A. Buck, and A. F. Horwitz. 1985. Distribution of the cell substratum attachment (CSAT) antigen on myogenic and fibroblastic cells in culture. *J. Cell Biol.* 100:1528-1539.
18. Denning, G. M., I. S. Kim, and A. B. Fulton. 1988. Shedding of cytoplasmic actins by developing muscle cell. *J. Cell Sci.* 89:273-282.
19. DePasquale, J. A., and C. S. Izzard. 1991. Accumulation of talin in nodes at the edge of the lamellipodium and separate incorporation into adhesion plaques at focal contacts in fibroblasts. *J. Cell Biol.* 113:1351-1359.
20. Dingus, J., S. Hwo, and J. Bryan. 1986. Identification by monoclonal antibodies and characterization of human platelet caldesmon. *J. Cell Biol.* 102:1748-1757.
21. Dlugosz, A., P. Antin, V. Nachmias, and H. Holtzer. 1984. The relationship between stress fiber-like structures and nascent myofibrils in cultured cardiac myocytes. *J. Cell Biol.* 99:2268-2278.
22. Eldridge, J., A. Aehner, and B. M. Paterson. 1985. Nucleotide sequence of the chicken cardiac alpha actin gene: absence of strong homologies in the promoter and 3'-untranslated regions with the skeletal alpha actin sequence. *Genetics.* 36:55-63.
23. Endo, T., and T. Masaki. 1984. Differential expression and distribution of chicken skeletal and smooth-muscle type α-actinins during myogenesis in culture. *J. Cell Biol.* 99:2322-2332.
24. Forbes, M. S., and N. Sperelakis. 1985. Intercalated discs of mammalian heart: a review of structure and function. *Tissue & Cell.* 17:605-648.
25. Fuerst, D. O., R. Nave, M. Osborn, and K. Weber. 1989. Repetitive titin epitopes with a 42 nm spacing coincide in relative position with known

A band striations also identified by major myosin-associated proteins. *J. Cell Sci.* 94:119-125.

26. Geiger, B. 1983. Membrane-cytoskeleton interaction. *Biochim. Biophys. Acta.* 737:305-341.

27. Geiger, B., Z. Avnur, T. E. Kreis, and J. Schlessinger. 1984. The dynamics of cytoskeletal organization in areas of cell contact. *Cell Muscle Motil.* 5:195-234.

28. Geiger, B., T. Volk, T. Volberg, and R. Bendori. 1987. Molecular interactions in adherens-type contacts. *J. Cell Sci. Suppl.* 8:251-272.

29. Handel, S. E., M. L. Greaser, E. Schultz, S.-M. Wang, J. C. Bulinski, J. J.-C. Lin, and J. L. Lessard. 1991. Chick cardiac myofibrillogenesis studied with antibodies specific for titin and the muscle and nonmuscle isoforms of actin and troponin. *Cell Tissue Res.* 263:419-430.

30. Hayward, L. J., and R. J. Schwartz. 1986. Sequential expression of chick actin genes during myogenesis. *J. Cell Biol.* 102:1485-1493.

31. Holtzer, H., J. Marshall, and H. Finck. 1957. An analysis of myogenesis by the use of fluorescent antimyosin. *J. Biophys. Biochem. Cytol.* 3:705-723.

32. Holtzer, H., T. Schultheiss, C. DiLullo, J. Choi, M. Costa, M. Lu, and S. Holtzer. 1990. Autonomous expression of the differentiation programs of cells in the cardiac and skeletal myogenic lineages. *Ann. NY Acad. Sci.* 599:158-169.

33. Ishikawa, H., R. Bischoff, and H. Holtzer. 1969. Formation of arrowhead complexes with heavy meromyosin in a variety of cell types. *J. Cell Biol.* 43:312-328.

34. Izzard, C. S. 1988. A precursor of the focal contact in cultured fibroblasts. *Cell Motil. Cytoskeleton.* 10:137-142.

35. Jaken, S., K. Leach, and T. Klauck. 1989. Association of type 3 protein kinase C with focal contacts in rat embryo fibroblasts. *J. Cell Biol.* 109:697-704.

36. Jones, P., P. Jackson, G. Price, B. Patel, A. Lear, and D. Critchley. 1989. Identification of a talin binding site in the cytoskeletal protein vinculin. *J. Cell Biol.* 109:2917-2927.

37. Kolega, J., L. Janson, and D. Taylor. 1991. The role of solation-contraction coupling in regulating stress fiber dynamics in nonmuscle cells. *J. Cell Biol.* 114:993-1003.

38. Kratwetz, S. A., and R. A. Anwar. 1984. Optimization of the isolation of biologically active mRNA from chick embryo aorta. *Biotechniques.* 6:342-347.

39. Lazarides, E., and K. Burridge. 1975. α-actinin: immunofluorescent localization of a muscle structural protein in non-muscle cells. *Cell.* 6:289-298.

40. Lessard, J. L. 1988. Two monoclonal antibodies to actin: one generally reactive and the other muscle selective. *Cell Motil. Cytoskeleton.* 10:349-362.

41. Lin, Z., J. R. Eshelman, S. Forry-Schaudies, S. Duran, J. L. Lessard, and H. Holtzer. 1987. Sequential disassembly of myofibrils induced by myristate acetate in cultured myotubes. *J. Cell Biol.* 105:1365-1376.

42. Lin, Z., S. Holtzer, T. Schultheiss, J. Murray, T. Masaki, D. A. Fischman, and H. Holtzer. 1989. Polygons and adhesion plaques and the disassembly and assembly of myofibrils in cardiac myocytes. *J. Cell Biol.* 108:2355-2367.

43. Lubit, B. W., and J. H. Schwartz. 1980. An anti-actin antibody that distinguishes between cytoplasmic and skeletal muscle actins. *J. Cell Biol.* 86:891-897.

44. Noegel, A., and M. Schleicher. 1991. Phenotypes of cells with cytoskeletal mutations. *Curr. Opin. Cell Biol.* 3:18-26.

45. Otey, C. A., M. H. Kalnoski, J. L. Lessard, and J. C. Bulinski. 1986. Immunolocalization of the gamma isoform of nonmuscle actin in cultured cells. *J. Cell Biol.* 102:1726-1737.

46. Otto, J. J. 1990. Vinculin. *Cell Motil. Cytoskeleton.* 16:1-6.

47. Pardo, J. V., J. D. Siliciano, and S. W. Craig. 1983. Vinculin is a component of an extensive network of myofibril-sarcolemma attachment regions in cardiac muscle fibers. 97:1081-1088.

48. Pardo, J. V., M. F. Pittenger, and S. W. Craig. 1983. Subcellular sorting of isoactins: selective association of γ actin with skeletal muscle mitochondria. *Cell.* 32:1093-1103.

49. Pasdar, M., and W. J. Nelson. 1988. Kinetics of desmosome assembly in Madin-Darby Canine kidney epithelial cells: temporal and spatial regulation of desmoplakin organization and stabilization upon cell-cell contact. II. Morphological analysis. 106:687-695.

50. Pavalko, F., and K. Burridge. 1991. Disruption of the actin cytoskeleton after microinjection of proteolytic fragments of α-actinin. *J. Cell Biol.* 114:481-491.

51. Rubinstein, P., T. Rupper, and A. Sandra. 1982. Selective isoactin release from cultured embryonic skeletal muscle cells. *J. Cell Biol.* 92:164-169.

52. Ruzicka, D. L., and R. J. Schwartz. 1988. Sequential activation of α-actin genes during avian cardiogenesis: vascular smooth muscle α-actin gene transcripts mark the onset of cardiomyocte differentiation. *J. Cell Biol.* 107:2575-2586.

53. Sanger, J., B. Mittal, T. Meyer, and J. Sanger. 1989. Use of fluorescent probes to study myofibrillogenesis. *In* Cellular and Molecular Biology of Muscle Development. L. Kedes and F. Stockdale, editors. 221-235.

54. Schultheiss, T., Z. Lin, M.-H. Lu, J. Murray, D. A. Fischman, K. Weber, T. Masaki, M. Imamura, and H. Holtzer. 1990. Differential distribution of subsets of myofibrillar proteins in cardiac nonstriated and striated myofibrils. *J. Cell Biol.* 110:1159-1172.

55. Terai, M., M. Komiyama, and Y. Shimada. 1989. Myofibril assembly is linked with vinculin, a-actinin, and cell-substrate contacts in embryonic cardiac myocytes in vitro. *Cell Motil. Cytoskeleton.* 12:185-194.

56. Tidball, J. G. 1987. Alpha-actinin is absent from the terminal segments of myofibrils and from subsarcolemmal densities in frog skeletal muscle. *Exp. Cell Res.* 170:469-482.

57. Toyama, Y., S. Forry-Schaudies, B. Hoffman, and H. Holtzer. 1982. Effects of taxol and colcemid on myofibrillogenesis. *Proc. Natl. Acad. Sci. USA.* 79:6556-6560.

58. Tsukita, S., Y. Hieda, and S. Tsukita. 1989. A new 82-kD barbed end-capping protein (Radixin) localized in the cell-to-cell adherens junction: purification and characterization. *J. Cell Biol.* 108:2369-2382.

59. Turner, C. E., J. R. Glenney, Jr., and K. Burridge. 1990. Paxillin: a new vinculin-binding protein present in focal adhesions. *J. Cell Biol.* 111:1059-1068.

60. Volk, T., and B. Geiger. 1986. A-CAM: a 135-kD receptor of intracellular adherens junctions. I. Immunoelectron microscopic localization and biochemical studies. *J. Cell Biol.* 103:1441-1450.

61. Wang Y.-L. 1984. Reorganization of actin filament bundles in living fibroblasts. *J. Cell Biol.* 99:1478-1485.